A simple artificial light-harvesting dyad as a model for excess energy dissipation in oxygenic photosynthesis

Rudi Berera[†], Christian Herrero[‡], Ivo H. M. van Stokkum[†], Mikas Vengris[†], Gerdenis Kodis[‡], Rodrigo E. Palacios[‡], Herbert van Amerongen[§], Rienk van Grondelle[†], Devens Gust[‡], Thomas A. Moore[‡], Ana L. Moore[‡], and John T. M. Kennis[†¶]

[†]Department of Biophysics, Division of Physics and Astronomy, Faculty of Sciences, Vrije Universiteit, 1081 HV, Amsterdam, The Netherlands; [‡]Department of Chemistry and Biochemistry and Center for the Study of Early Events in Photosynthesis, Arizona State University, Tempe, AZ 85287; and [§]Laboratory for Biophysics, Wageningen University, 6703 HA, Wageningen, The Netherlands

Edited by Robin M. Hochstrasser, University of Pennsylvania, Philadelphia, PA, and approved February 10, 2006 (received for review September 29, 2005)

Under excess illumination, plant photosystem II dissipates excess energy through the quenching of chlorophyll fluorescence, a process known as nonphotochemical quenching. Activation of nonphotochemical quenching has been linked to the conversion of a carotenoid with a conjugation length of nine double bonds (violaxanthin) into an 11-double-bond carotenoid (zeaxanthin). It has been suggested that the increase in the conjugation length turns the carotenoid from a nonquencher into a quencher of chlorophyll singlet excited states, but unequivocal evidence is lacking. Here, we present a transient absorption spectroscopic study on a model system made up of a zinc phthalocyanine (Pc) molecule covalently linked to carotenoids with 9, 10, or 11 conjugated carbon–carbon double bonds. We show that a carotenoid can act as an acceptor of Pc excitation energy, thereby shortening its singlet excited-state lifetime. The conjugation length of the carotenoid is critical to the quenching process. Remarkably, the addition of only one double bond can turn the carotenoid from a nonquencher into a very strong quencher. By studying the solvent polarity dependence of the quenching using target analysis of the time-resolved data, we show that the quenching proceeds through energy transfer from the excited Pc to the optically forbidden S_1 state of the carotenoid, coupled to an intramolecular charge-transfer state. The mechanism for excess energy dissipation in photosystem II is discussed in view of the insights obtained on this simple model system.

artificial photosynthesis | carotenoid | nonphotochemical quenching | photoprotection | xanthophyll cycle

The ubiquity of carotenoids in nature reflects the crucial roles they play. In photosynthesis, carotenoids act mainly as light harvesters and photoprotectors. They absorb light in the blue-green region, where chlorophylls (Chls) display little absorption and transfer the energy to neighboring Chls (1, 2), thus increasing the absorption cross section for photosynthesis. Their role in the photoprotection of the photosynthetic apparatus is of vital importance; carotenoids can both scavenge injurious singlet oxygen and prevent its sensitization by quenching the Chl triplet state (3). Another crucial function of carotenoids, extensively studied yet poorly understood at the molecular level, is their role in the quenching of Chl singlet excited states in photosystem II (PSII) under excess illumination (4–7). This process, known as nonphotochemical quenching, allows the plant to adapt to different light levels by preventing photoinduced damage (8). Feedback deexcitation is the main component of nonphotochemical quenching (7, 9). Its activation and regulation is linked to an enzymatic, rapidly reversible process known as the xanthophyll cycle. Under high light illumination a drop in the thylakoid lumen pH triggers the cycle: violaxanthin, a 9-double-bond carotenoid, is converted into zeaxanthin, an 11-double-bond carotenoid (7). As the intensity of light decreases, or under conditions of dim light, the process is reversed. Besides activating the xanthophyll cycle, the drop in luminal pH leads to protonation of PsbS (10), a PSII subunit thought to have a central role in feedback deexcitation (11).

The question of whether zeaxanthin plays a direct role in the quenching process remains unsettled. It has been proposed that expanding the conjugation length from 9 to 11 double bonds brings the energy level of the carotenoid S_1 state below that of the Q_y state of Chl, rendering the carotenoid capable of quenching the Chl excited state by energy transfer (12). The expansion of the conjugation length would lower the first oxidation potential of the carotenoid as well (13, 14), and thus quenching could also proceed by electron transfer (5, 12, 15, 16). Alternatively, it was suggested that structural differences between violaxanthin and zeaxanthin change the way the carotenoid interacts with the surrounding pigment–protein complex, leading to a change in the pigment organization that induces quenching (4, 5, 17). Even with the emergence of new crystallographic structures of the PSII antenna (18, 19), the role of zeaxanthin in nonphotochemical quenching remains unresolved.

Artificial light-harvesting antennae are used for the study of light harvesting, energy transfer, electron transfer, and photoprotective functions of carotenoids (20, 21). These minimalist constructs are capable of performing the specific functions carried out by their natural counterparts; their simplicity allows one to establish the basic photophysical and photochemical mechanisms underlying the behavior of the natural systems. Here, we present results from transient absorption spectroscopy on dyads consisting of a zinc phthalocyanine (Pc), acting as a mimick for Chl *a*, covalently linked to a series of carotenoids having 9, 10, or 11 conjugated carbon–carbon double bonds. These dyads have previously been shown to exhibit an efficient carotenoid-to-Pc light-harvesting function (22). We define the conditions under which a carotenoid molecule quenches the excited state of a Pc-based tetrapyrrole, identify the quenching mechanism, and determine to what extent the quenching depends on the conjugation length. The implications for the mechanism of excess energy dissipation in PSII are discussed.

Results

The structures of dyads **1**, **2**, and **3**, are shown in Fig. 1 *Upper*, and their absorption spectra along with that of model Pc **4** dissolved

Conflict of interest statement: No conflicts declared.

This paper was submitted directly (Track II) to the PNAS office.

Freely available online through the PNAS open access option.

Abbreviations: EADS, evolution-associated difference spectrum; SADS, species-associated difference spectrum; Pc, phthalocyanine; ICT intramolecular charge transfer; Chl, chlorophyll; PSII, photosystem II; THF, tetrahydrofuran; LHC, light-harvesting complex.

¶To whom correspondence should be addressed. E-mail: j.kennis@few.vu.nl.

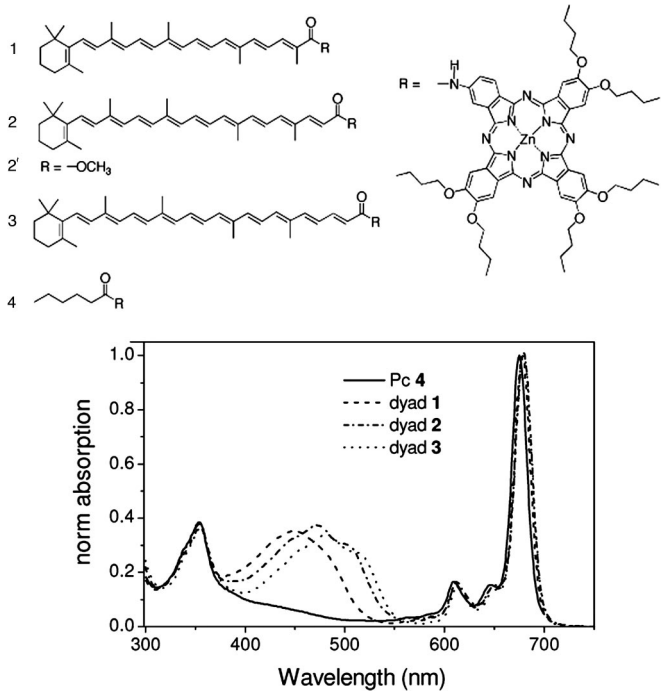

Fig. 1. Molecular structures and absorption spectra of the compounds. (*Upper*) Molecular structures of the dyads. A zinc-Pc is covalently linked to a carotenoid with 9 conjugated carbon–carbon double bonds (dyad **1**), 10 carbon–carbon double bonds (dyad **2**), and 11 carbon–carbon double bonds (dyad **3**). Model Pc **4** bears a hexanoyl group instead of a polyene. Model carotenoid **2**′ has a terminal ester instead of a Pc. (*Lower*) Absorption spectrum in THF for dyad **1** (dashed line), dyad **2** (dashed-dotted line), dyad **3** (dotted line), and model Pc **4** (solid line).

in tetrahydrofuran (THF) are shown in Fig. 1 *Lower*. The carotenoids of dyad **1**, **2**, and **3** have 9, 10, and 11 conjugated carbon–carbon double bonds, respectively, and a carbonyl group terminating the conjugated system. The carbonyl group is in an s-*cis* conformation, which only partly adds to π-conjugation of the system (1, 23). The lifetimes of the optically forbidden S_1 state of the model carotenoids of dyads **1** and **2**, determined previously to be 25 and 11.5 ps, respectively (21), are similar to those typically observed for other carotenoids with 9 and 10 conjugated carbon–carbon double bonds (1).

Fig. 2*A* shows kinetic traces with excitation and detection at 680 nm, corresponding to the maximum of Pc Q_y absorption, for dyads **1**–**3** and model Pc **4** dissolved in THF. The switch from nonquenching to quenching upon an increase in the conjugation length by one double bond is clearly seen in the shortened recovery time for the Pc ground-state bleach in dyad **2**. The lifetimes of the Q_y states in dyad **1** and model Pc **4** have the same value (3 ns), whereas for dyad **2** the lifetime is reduced by a factor of 10 to 300 ps. When the conjugation length of the carotenoid is further increased (dyad **3**) the carotenoid becomes an even stronger quencher, the lifetime of the Q_y state being 56 ps. Fig. 2 *B*–*D* shows the results (see below).

Dyad 1. The results of a global analysis of the time-resolved data taken on dyad **1** are presented as evolution-associated difference spectra (EADS) in Fig. 2*B*. Four kinetic components are needed for an adequate description: the first, appearing at time 0 and evolving into the second in 100 fs, is mainly the consequence of cross-phase modulation and coherent artifacts and is not shown. The second EADS (Fig. 2*B*, red line) has a lifetime of 1.25 ps and features ground-state bleach in the Q_x band of Pc (610 nm), ground-state bleach and stimulated emission in the Q_y band of

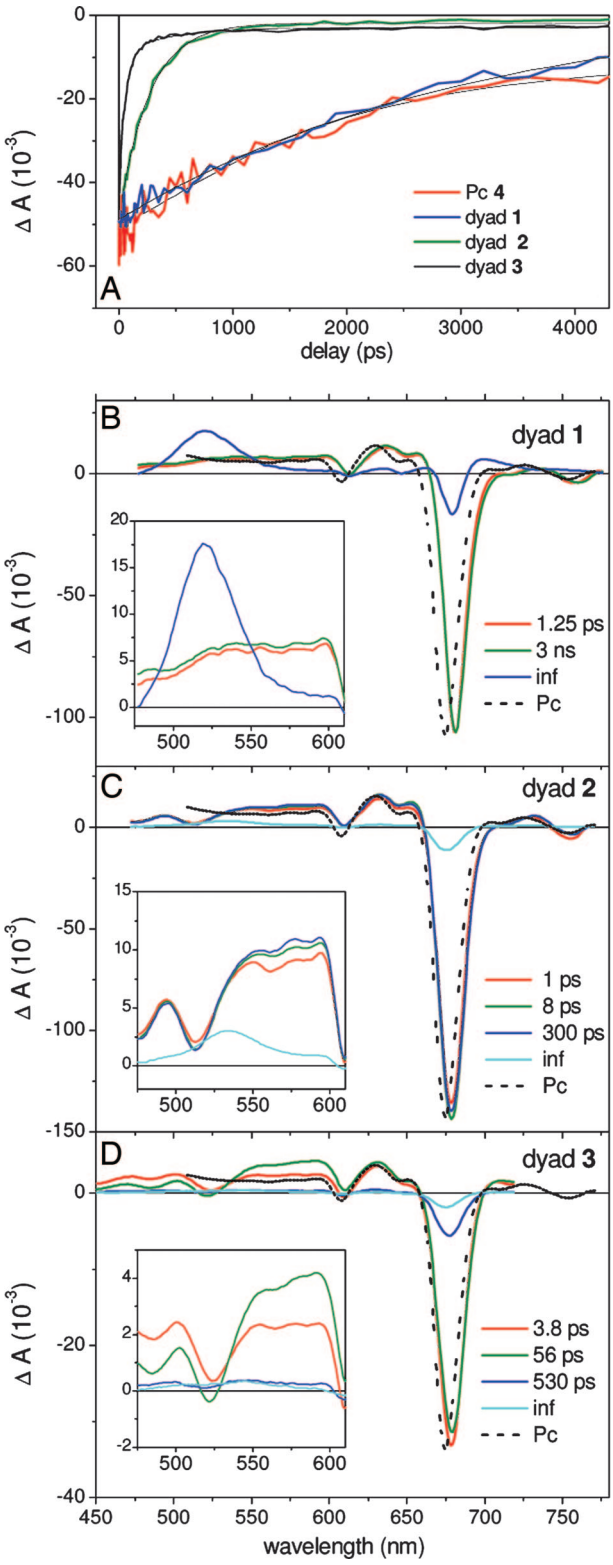

Fig. 2. Kinetic traces and global analysis of the time-resolved data. (*A*) Kinetic traces with excitation and detection at 680 nm for model Pc **4** (red line), dyad **1** (blue line), dyad **2** (green line), and dyad **3** (magenta line) in THF, along with the result of the global analysis fit (thin solid line). (*B*) EADS that follow from a global analysis of data for dyad **1**. (*Inset*) An expanded view of the EADS in the spectral region from 475 to 620 nm. (*C*) The same as for *B* for dyad **2**. (*D*) The same as for B for dyad **3**. The difference spectra corresponding to the vibrationally relaxed, fully solvated Q_y state for model Pc **4**, as determined from a global analysis, are also shown in *B*–*D* as black dashed lines.

Pc (680 nm), stimulated emission from Q_y (≈750 nm), and a broad, flat excited-state absorption from 480 to 600 nm. It evolves to the next EADS (Fig. 2*B*, green line), involving minor spectral changes, including a slight red shift of the Q_y bleach/stimulated emission signal near 680 nm, which is probably caused by solvation processes. The third EADS evolves into the nondecaying fourth EADS (Fig. 2*B*, blue line) in 3 ns. At this stage the Pc transient signals have greatly decreased. The spectrum presents a new absorption band near 515 nm corresponding to a carotenoid triplet excited state, as observed previously in a carotenoid–Si–Pc triad containing the same carotenoid (21). This feature is absent in the previous EADS and appears after most Pc has returned to the ground state. This observation suggests that carotenoid triplet formation is preceded by singlet to triplet intersystem crossing in Pc, followed by rapid triplet–triplet energy transfer between Pc and the carotenoid. The signal in the Q_y region of Pc has the typical shape of a band shift, as previously observed in the Si-Pc triads (21). When comparing the shape and amplitude of the first two EADS (Fig. 2*B*, red and green lines) with the spectrum corresponding to the vibrationally relaxed and fully solvated excited state of model Pc **4** (Fig. 2*B*, dashed black line), apart from an overall spectral shift and a more pronounced excited-state absorption shoulder at 655 nm in the dyad, there are only minor differences. Furthermore, the lifetime of the Q_y state of dyad **1** (3 ns) differs only marginally from the excited-state lifetime for model Pc **4**, meaning that the carotenoid in dyad **1** is incapable of quenching the Pc excited singlet state.

Dyad 2. Fig. 2*C* shows the EADS for dyad **2**. Five components are needed for a satisfactory fit. The first component, appearing at time 0 and evolving into the second spectrum in 100 fs, is again not shown. The second EADS (Fig. 2*C*, red line) has a lifetime of 1 ps and is similar to the corresponding EADS in dyad **1**. However, it also presents a small negative feature near 515 nm superimposed on the broad excited-state absorption signal that is absent in the spectra of model Pc **4** and dyad **1**. This phenomenon, highlighted in the Fig. 2*C Inset*, occurs in the ground-state absorption region of the covalently linked carotenoid and appears to be a band shift, possibly in combination with a small bleach of the carotenoid ground-state absorption, and results from excitation of Pc. This feature is similar to that observed previously in photosynthetic light-harvesting complexes (LHCs), where it was assigned to a change of the local electric field of the carotenoid and excitonic coupling between Chl and the optically allowed S_2 state of the carotenoid (24, 25). The second EADS evolves into the third EADS (Fig. 2*C*, green line) in 1 ps, with only minor changes in the shape and amplitude of the spectrum. There is a slight increase of the signal near 680 nm and a very small increase of the excited-state absorption in the 550- to 600-nm region. The evolution to the fourth EADS (Fig. 2*C*, blue line) occurs in 8 ps. This EADS is almost identical to the previous one apart from a very small decrease of the Q_y bleach. The fourth EADS evolves into the nondecaying fifth EADS (Fig. 2*C*, cyan line) in 300 ps. Now the Pc bleach and excited-state features have almost disappeared. The nondecaying EADS is characterized by a small residual bleach in the Q_y region and a small, broad, positive signal in the 500- to 580-nm region, corresponding to carotenoid triplet, and possibly Pc triplets. A crucial difference between these results and those of dyad **1** is the lifetime of the Pc singlet excited state. This value, 300 ps for dyad **2**, is 10 times shorter than in dyad **1** and model Pc **4**, meaning that the carotenoid of dyad **2** acts as a strong, effective quencher of Pc singlet excited states.

Dyad 3. The EADS for dyad **3** are presented in Fig. 2*D*. Again, the first EADS, with a lifetime of 100 fs, is not shown. The second EADS (Fig. 2*D*, red line) displays Q_x and Q_y bleach at 610 and 680 nm, respectively, and excited-state absorption features similar to those observed for dyads **1** and **2**. At 525 nm there is a negative-going feature, similar to that observed for dyad **2** but red-shifted by ≈10 nm. As in dyad **2**, we assign it to a band-shift/ground-state bleach of the carotenoid ground-state absorption upon excitation of Pc. The second EADS evolves into the third EADS (Fig. 2*D*, green line) in 3.8 ps. In the third EADS, a sizeable increase of the positive signal in the region above 540 nm is observed, as well as a small decrease of the Q_y bleach. In the region below 540 nm the third EADS shows a growth and blue shift of the negative feature, and, as mentioned above, an increase of the absorption at wavelengths >540 nm, as highlighted in Fig. 2*D Inset*. With a 56-ps time constant, this EADS evolves into the fourth one (Fig. 2*D*, blue line); the Q_y bleach and the excited-state absorption have dramatically decreased and most of Pc is now in its ground state. The remaining signal decays in 530 ps to the nondecaying component characterized by a small population of a long-lived, presumably triplet, species. In dyad **3** the Pc singlet lifetime is strongly quenched compared with dyads **1** and **4**. The decay of the Pc singlet excited state, as measured by Q_y bleach recovery, is biexponential with most of the excited states disappearing in 56 ps and a small fraction in 530 ps.

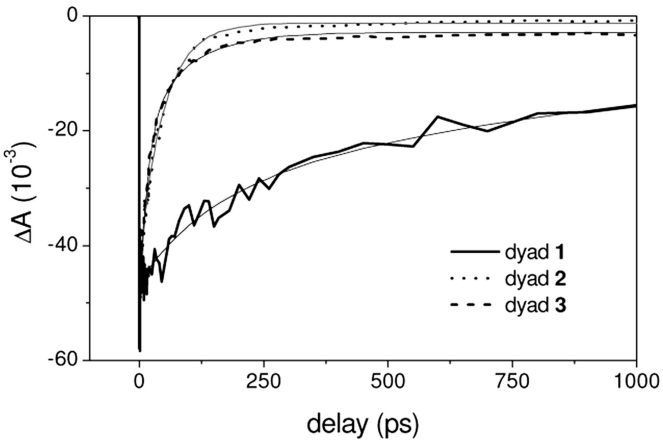

Fig. 3. Kinetic traces with excitation and detection at 680 nm for dyad **1** (solid line), dyad **2** (dotted line), and dyad **3** (dashed line) in acetone. The gray lines denote the result of a global analysis.

A closer look at the evolution from the second to the third EADS (Fig. 2*D*, red to green curve, in 3.8 ps) suggests that the increase of negative-going amplitude in the region <540 nm may correspond to depopulation of the carotenoid ground state, whereas the increase of the signal >540 nm must originate from the absorption of a species different from the Pc Q_y state (Fig. 2*D*, dashed black line). It will be later identified as a carotenoid excited state. This species appears to rise on a picosecond time scale and coexists from then on with the Pc Q_y state. This behavior suggests that the carotenoid state is slowly populated and quickly depopulated. Such a state may act as a quencher because its lifetime is far shorter than the intrinsic lifetime of the Pc Q_y state. For dyad **2**, similar phenomena appear to occur (Fig. 2*C Inset*) but are much less pronounced.

Solvent Polarity Dependence of Pc Singlet-Excited-State Quenching. To gain more insight into the quenching mechanism, we carried out experiments with dyads dissolved in acetone and DMSO. THF is of moderate polarity, with a static dielectric constant $\varepsilon_0 = 7.58$ and an index of refraction $n_D = 1.405$, whereas acetone ($\varepsilon_0 = 20.6$, $n_D = 1.356$) and DMSO ($\varepsilon_0 = 40.5$, $n_D = 1.478$) are of distinctly high polarity. Fig. 3 shows the kinetic traces and corresponding global analysis fits recorded at 680 nm for dyads

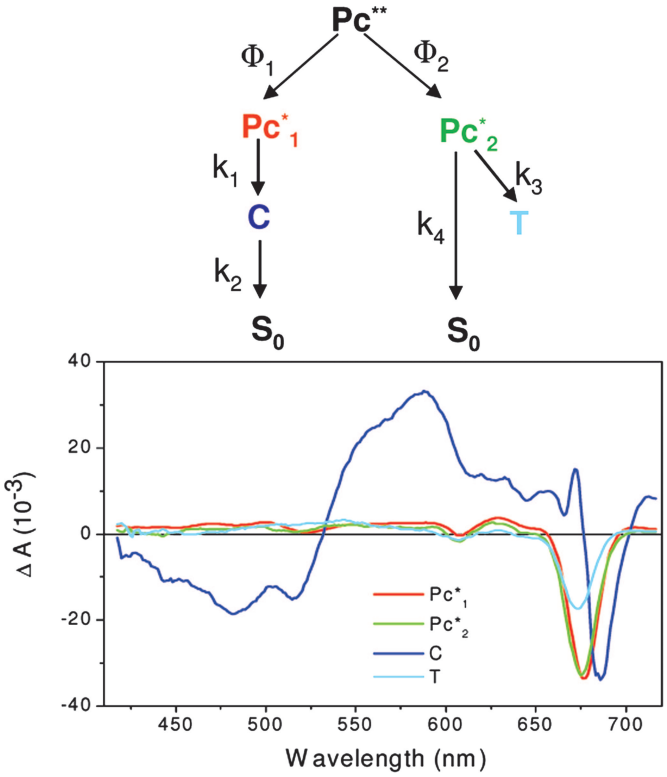

Fig. 4. Target analysis of the time-resolved data. (*Upper*) Kinetic model used in target analysis of time-resolved data on dyads **2** and **3**. (*Lower*) SADS from the target analysis for dyad **3** in THF. See text for details.

1–**3** in acetone. In all three systems the Q_y state has a shorter lifetime than it does in THF (Fig. 2*A*). Dyad **1** decayed monoexponentially with a time constant of 600 ps. Dyad **2** displayed a biexponential decay with time constants of 30 ps (75% amplitude) and 120 ps (25% amplitude), whereas dyad **3** showed a decay with 16 ps (65%) and 90 ps (35%). A similar scenario was found in DMSO (results not shown). Thus, in polar solvents the quenching becomes faster. The results from a global analysis on dyad **3** in acetone are shown in Fig. 6, which is published as supporting information on the PNAS web site.

Target Analysis: Identification of the Quenching Species. The sequential data analysis allows extraction of intrinsic lifetimes, but the spectra generally represent a mixture of transient species. Therefore, despite providing strong evidence for the presence of a transient species other than singlet-excited Pc, sequential analysis alone cannot provide a definitive spectral signature of such a species. To identify the relevant molecular states, we globally analyzed the time-resolved data with a target analysis, wherein the data are described in terms of a kinetic scheme, enabling the estimation of the spectral signatures, and lifetimes, of the "pure" molecular species (26). Our goal is to identify the carotenoid state that is responsible for quenching the singlet excited state of Pc.

The biexponential decay of Q_y in the case of dyad **3** observed in THF and acetone may stem from an inhomogeneity of the dyad ground-state population in which one species is more strongly quenched than the other. To account for the biexponentiality the target analysis model requires two independent Pc excited-state populations.

The kinetic model is depicted in Fig. 4 *Upper* and consists of five compartments: The first, **Pc****, corresponds to an unrelaxed Pc excited state that decays in <100 fs into two independent Pc excited-state populations, $\mathbf{Pc}_1^*$ and $\mathbf{Pc}_2^*$ (target analysis cannot distinguish this case from the case of two unrelaxed Pc excited-state species prepared initially). A fraction Φ_1 relaxes to $\mathbf{Pc}_1^*$, whereas a fraction Φ_2 relaxes to $\mathbf{Pc}_2^*$. $\mathbf{Pc}_1^*$ evolves to **C**, which represents a carotenoid state, with a rate constant k_1. **C** decays entirely to the ground state with a rate constant k_2. In this model the carotenoid state **C** is slowly populated and quickly depopulated and therefore attains a low transient concentration. $\mathbf{Pc}_2^*$ decays with rate constant k_3 to a long-lived mix of Pc and carotenoid triplet states **T**, in competition with decay to the ground state with a rate constant k_4.

Fig. 4 *Lower* shows the species-associated difference spectra (SADS) resulting from target analysis for dyad **3** in THF. The estimated rate constants and branching ratios are summarized in Table 1. The spectrum corresponding to **Pc**** is not shown; 82% of **Pc**** decays to $\mathbf{Pc}_1^*$ (Fig. 4 *Lower*, red line), whereas 18% decays to $\mathbf{Pc}_2^*$ (Fig. 4 *Lower*, green line). $\mathbf{Pc}_1^*$ decays to **C** (Fig. 4 *Lower*, blue line) with a rate constant of $(56\ \text{ps})^{-1}$, which in turn decays to the ground state with a rate constant $(3.8\ \text{ps})^{-1}$. $\mathbf{Pc}_2^*$ decays to **T** (Fig. 4 *Lower*, cyan line) with a rate constant of $(840\ \text{ps})^{-1}$ and to the ground state with a rate constant of $(1.3\ \text{ns})^{-1}$. The SADS (Fig. 4) of $\mathbf{Pc}_1^*$ shows bleaching of the Q_x and Q_y bands and a broad excited-state absorption from 520 to 600 nm. Compared with the EADS with a lifetime of 56 ps in Fig. 2*D* (green line), the carotenoid bleach feature near 520 nm and absorption feature near 550 nm have largely disappeared, indicating that the separation of Pc and carotenoid signals was successful. The small carotenoid band-shift/ground-state bleach remains present in the $\mathbf{Pc}_1^*$ SADS, consistent with its instantaneous occurrence in the sequential analysis.

The SADS of state **C** has the typical shape of the $S_1 \rightarrow S_n$ transient absorption spectrum of carotenoids (1). The negative features at wavelengths <530 nm correspond to ground-state bleaching of the strongly allowed S_2 state, with vibronic features at 480 and 520 nm. The excited-state absorption region >530 nm is typical for the S_1 state with a maximum at 580 nm and a pronounced shoulder near 550 nm. The strong bleach in the 680- to 690-nm region is an artifact and forms no part of the carotenoid S_1 spectrum. It results from relaxation processes of Pc that take place on the ps time scale and are independent from the quenching phenomenon, but could not be separated from the carotenoid dynamics in the target analysis procedure. In reality, this feature represents a small red shift of the Pc bleach, also observed in model Pc **4** (data not shown), and is artificially expanded by the target analysis. The results for dyad **2** and **3** in acetone are shown in Fig. 7, which is published as supporting

Table 1. Rate constants for dyad 3 in THF and dyads 2 and 3 in acetone as derived from the target kinetic model depicted in Fig. 4

Compound, solvent	Φ_1	Φ_2	k_1	k_2	k_3	k_4
Dyad **3**, THF	0.82	0.18	$(56\ \text{ps})^{-1}$	$(4\ \text{ps})^{-1}$	$(840\ \text{ps})^{-1}$	$(1.3\ \text{ns})^{-1}$
Dyad **2**, acetone	0.75	0.25	$(30\ \text{ps})^{-1}$	$(4\ \text{ps})^{-1}$	$(526\ \text{ps})^{-1}$	$(179\ \text{ps})^{-1}$
Dyad **3**, acetone	0.54	0.46	$(17\ \text{ps})^{-1}$	$(4.8\ \text{ps})^{-1}$	$(303\ \text{ps})^{-1}$	$(130\ \text{ps})^{-1}$

Φ_1 and Φ_2 are population fractions at the branching point.

information on the PNAS web site. We attempted to apply the target analysis to dyad **2** dissolved in THF, but found that the transient concentration of excited-state carotenoid species **C** was too low to reliably estimate its spectral shape and dynamics.

The polarity dependence of the quenching suggests that electron transfer from the carotenoid to the Pc moiety could be responsible for the quenching process. To test this possibility we extensively probed the 850- to 980-nm region, but did not find any signature of a carotenoid radical ion (see Fig. 8, which is published as supporting information on the PNAS web site). In all systems, including model **4**, we found the same scenario: a relatively flat spectrum decaying with the same lifetime as the Q_y state of Pc, confirming that the signal in this region is entirely caused by Pc excited-state absorption.

By showing that the SADS of the quenching species strongly resembles that of the well known S_1 difference spectrum of carotenoids (1), target analysis provides good evidence for the essential role of the carotenoid S_1 excited state as an energy acceptor in the quenching process. However, because energy transfer to or from the S_1 state should not depend markedly on solvent polarity (1), simple energy transfer involving the unperturbed carotenoid S_1 state is unlikely to be solely responsible for the Pc excited-state quenching. To characterize the putative perturbation to S_1, we performed transient absorption measurements on a model for the carotenoid from dyad **2**, where Pc was replaced by a methyl ester (Fig. 1, model carotenoid **2′**), dissolved in solvents of different polarities. Fig. 9, which is published as supporting information on the PNAS web site, shows the EADS of the model carotenoid after internal conversion from S_2 in ≈100 fs and vibrational cooling in ≈500 fs, dissolved in DMSO (green curve), THF (blue curve), and hexane (red curve). Solvent polarity-dependent shape changes that cannot be ascribed to the unperturbed S_1 state are readily apparent. In hexane the spectrum looks like the well known difference spectrum associated with population of the S_1 state of carotenoids (1), but in THF a new band, characterized by a broad signal in the region >625 nm, is present. When the polarity is further increased (DMSO), this signal (>650 nm) becomes more prominent.

A similar dependence of spectral shape on solvent polarity was reported for several naturally occurring substituted carotenoids and assigned to the formation of an intramolecular charge transfer (ICT) state (23, 27). The ICT state is thought to arise from the presence of a carbonyl moiety in conjugation with the extended π-electron system; the carbonyl moiety accumulates electron density upon photoexcitation. The ICT and S_1 states may effectively behave as one state (27) or as distinct molecular states that equilibrate rapidly upon population from the optically allowed S_2 state (28). The carotenoids in this study also feature carbonyl groups. In model carotenoid **2′**, the presence of a charge transfer band coexisting with the S_1 state is clear. The spectral signature of the carotenoid state **C** as it follows from the target analysis (Fig. 4 *Lower*) and Fig. 7 shows a broad, flat excited-state absorption at wavelengths longer than ≈600 nm, which is consistent with the population of an ICT state in this system as well. Thus, the quenching state in the dyads most likely does not correspond to the pure S_1 state, but to a mixture of S_1 and ICT states. Note that because ICT and S_1 are closely linked, it is not possible to treat them as separate entities in the target analysis.

Discussion

A change in the conjugation length of carotenoids is a key characteristic of the process leading to the thermal dissipation of excess energy in PSII, where the activation of Chl singlet excited-state quenching is correlated with the conversion of violaxanthin (nine double bonds) into zeaxanthin (11 double bonds). Our results with artificial light-harvesting dyads show

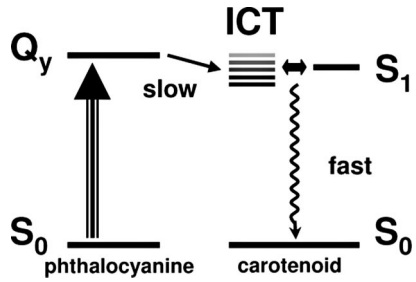

Fig. 5. Schematic representation of the proposed quenching process: the energy from the Q_y state of Pc is transferred to the carotenoid ICT state, which then equilibrates with the carotenoid S_1 state before relaxation to the ground state by internal conversion. An increase in solvent polarity leads to a lowering of the ICT energy (gray to black lines).

that a carotenoid of proper length can efficiently dissipate the Q_y energy of Pc by shortening its excited-state lifetime. In THF, a solvent of moderate polarity, an increase of the conjugation length by one double bond (dyad **1** to dyad **2**) turns the carotenoid from a nonquencher into a strong quencher. When the molecules are dissolved in the highly polar solvents acetone and DMSO, the quenching becomes stronger and even dyad **1** displays limited quenching. Target analysis has shown that the quenching in dyads **2** and **3** proceeds via a carotenoid S_1/ICT state. The solvent polarity dependence indicates that the ICT state modulates the process as shown in Fig. 5. The Q_y state of Pc transfers energy to the ICT state, which quickly equilibrates with S_1. Then, the carotenoid rapidly relaxes to the ground state on the time scale of several picoseconds by internal conversion. The increase in solvent polarity shifts the energy of the ICT state downward (Fig. 5, gray to black lines), making it more accessible from the Q_y state of Pc and increasing the quenching.

ICT states are not confined to carotenoids that have a carbonyl group in their conjugated system, as there is evidence for their occurrence in xanthophylls bound to natural photosynthetic LHCs, in particular LHCII, the main constituent of the PSII antenna (29). Instead of an internal electron withdrawing group (such as a carbonyl), the interaction with polar amino acids, inorganic cations such as Mg^{2+} or nearby pigments, resulting in a highly asymmetric environment of the molecule, may stabilize an ICT state. Also, geometric deformations of the polyene backbone have been proposed to play a role in lowering ICT states in carotenoids (30). Trimeric LHCII binds two luteins that are distinguishable by their steady-state absorption spectrum. A red-shifted lutein shows a particularly large Stark effect with a $|\Delta\mu|$ of 14.6 D (29), which corresponds to the transfer of ≈12% of an elementary charge along the conjugated backbone (31), demonstrating that electronic excited states in xanthophylls can be strongly coupled to ICT states. Interestingly, neither the second, blue-shifted lutein in trimeric LHCII, nor either of the two luteins in monomeric LHCII exhibited such a pronounced Stark effect. Additionally, it was shown that the red-shifted lutein assumed a distorted geometry in LHCII trimers, whereas the blue lutein assumes a relaxed conformation (32). These observations indicate that very specific carotenoid–protein or carotenoid–Chl interactions are responsible for the mixing between lutein electronic excited and ICT states, induced by conformational changes of the highly plastic LHCII protein.

It has been argued that the quenching of Chl excited states by zeaxanthin in PSII could not occur via the zeaxanthin S_1 state because the S_1 energies of violaxanthin and zeaxanthin in organic solvent and recombinant LHCII are not sufficiently different and lie below that of Chl *a* (6, 33, 34). However, *in vivo* light absorption and resonant Raman experiments on quenched PSII in leaves and chloroplasts indicated that zeaxanthin undergoes

dramatic spectroscopic changes upon induction of feedback deexcitation: its absorption maximum shifts to the red by at least 22 nm, and the molecule assumes a very specific, highly twisted conformation (35). To account for these phenomena, Ruban *et al.* (35) proposed that zeaxanthin is bound in a highly polarizing local environment, possibly arising from a strong electric field of a dipole or charge in the zeaxanthin vicinity. It seems plausible that such an extensive change of local environment, combined with a distortion of the polyene backbone, may bring down ICT states of zeaxanthin to couple with S_1, and thereby activate a quenching mechanism similar to that reported here for the model systems.

Conclusions

Our results with covalently linked carotenoid–Pc dyads show that carotenoids can efficiently quench tetrapyrrole singlet excited states by means of singlet energy transfer to low-lying, optically forbidden carotenoid excited states. The solvent polarity dependence and spectroscopic evidence point to the involvement of a carotenoid ICT state in the energy transfer process. Moreover, expanding the conjugated system of a carotenoid by only one double bond turns the carotenoid from a nonquencher into an effective quencher of Pc singlet excited states. In the antenna of PSII, a similar phenomenon may take place where the addition of two double bonds to the conjugated system of violaxanthin converts it to zeaxanthin, which may be a strong quencher. In other caroteno-tetrapyrrole constructs having structures and thermodynamics for photoinduced electron transfer distinctly different from those of dyads **1–3** electron transfer quenching of the tetrapyrrole Q_y state has been unequivocally assigned (21, 36). Having these two model systems in hand, it should be possible to establish the factors controlling the quenching mechanisms in natural photosynthesis.

Materials and Methods

Synthesis of the dyads is described in *Supporting Text*, which is published as supporting information on the PNAS web site. Femtosecond transient absorption spectroscopy was carried out with a spectrometer as described earlier (37). The excitation was tuned to 680 nm to selectively excite the Q_y state of Pc. The pulse energy was 100 nJ, corresponding to an excitation density of $\approx 10^{15}$ photons·pulse^{-1}·cm^{-2}. The data were globally analyzed (26) by using a kinetic model consisting of sequentially interconverting EADS, e.g., $1 \rightarrow 2 \rightarrow 3 \rightarrow \ldots$ in which the arrows indicate successive monoexponential decays of increasing time constants, which can be regarded as the lifetime of each EADS. The number of kinetic components corresponds to the minimum required to eliminate any correlated structure in the residuals. The first EADS corresponds to the time-zero difference spectrum. Because the EADS may reflect mixtures of molecular species, a target analysis was performed in which a specific kinetic scheme was applied. With this procedure, the SADS of pure molecular states were estimated. The instrument response function was fitted to a Gaussian of 120 fs (full width at half maximum), similar to the value obtained from the analysis of the induced birefringence in CS_2.

R.B. was supported by the Netherlands Organization for Scientific Research through the Earth and Life Sciences Council (NWO-ALW). J.T.M.K. was supported by the NWO-ALW through a VIDI fellowship. This work was supported by Department of Energy Grant FG02-03ER15393. This is publication 659 from the Arizona State University Center for the Study of Early Events in Photosynthesis.

1. Polivka, T. & Sundström, V. (2004) *Chem. Rev.* **104,** 2021–2071.
2. Frank, H. A. & Cogdell, R. J. (1996) *Photochem. Photobiol.* **63,** 257–264.
3. Griffiths, M., Sistrom, W. R., Cohenbazire, G. & Stanier, R. Y. (1955) *Nature* **176,** 1211–1214.
4. Robert, B., Horton, P., Pascal, A. A. & Ruban, A. V. (2004) *Trends Plant Sci.* **9,** 385–390.
5. Holt, N. E., Fleming, G. R. & Niyogi, K. K. (2004) *Biochemistry* **43,** 8281–8289.
6. Frank, H. A., Bautista, J. A., Josue, J. S. & Young, A. J. (2000) *Biochemistry* **39,** 2831–2837.
7. Muller, P., Li, X. P. & Niyogi, K. K. (2001) *Plant Physiol.* **125,** 1558–1566.
8. Kulheim, C., Agren, J. & Jansson, S. (2002) *Science* **297,** 91–93.
9. Horton, P., Ruban, A. V. & Walters, R. G. (1996) *Annu. Rev. Plant Physiol. Plant Mol. Biol.* **47,** 655–684.
10. Li, X. P., Gilmore, A. M., Caffarri, S., Bassi, R., Golan, T., Kramer, D. & Niyogi, K. K. (2004) *J. Biol. Chem.* **279,** 22866–22874.
11. Li, X. P., Björkman, O., Shih, C., Grossman, A. R., Rosenquist, M., Jansson, S. & Niyogi, K. K. (2000) *Nature* **403,** 391–395.
12. Frank, H. A., Cua, A., Chynwat, V., Young, A., Gosztola, D. & Wasielewski, M. R. (1994) *Photosynth. Res.* **41,** 389–395.
13. Dreuw, A., Fleming, G. R. & Head-Gordon, M. (2003) *Phys. Chem. Chem. Phys.* **5,** 3247–3256.
14. Fungo, F., Otero, L., Durantini, E., Thompson, W. J., Silber, J. J., Moore, T. A., Moore, A. L., Gust, D. & Sereno, L. (2003) *Phys. Chem. Chem. Phys.* **5,** 469–475.
15. Ma, Y. Z., Holt, N. E., Li, X. P., Niyogi, K. K. & Fleming, G. R. (2003) *Proc. Natl. Acad. Sci. USA* **100,** 4377–4382.
16. Holt, N. E., Zigmantas, D., Valkunas, L., Li, X. P., Niyogi, K. K. & Fleming, G. R. (2005) *Science* **307,** 433–436.
17. Pascal, A. A., Liu, Z. F., Broess, K., van Oort, B., van Amerongen, H., Wang, C., Horton, P., Robert, B., Chang, W. R. & Ruban, A. (2005) *Nature* **436,** 134–137.
18. Liu, Z. F., Yan, H. C., Wang, K. B., Kuang, T. Y., Zhang, J. P., Gui, L. L., An, X. M. & Chang, W. R. (2004) *Nature* **428,** 287–292.
19. Standfuss, R., van Scheltinga, A. C. T., Lamborghini, M. & Kühlbrandt, W. (2005) *EMBO J.* **24,** 919–928.
20. Gust, D., Moore, T. A. & Moore, A. L. (2001) *Acc. Chem. Res.* **34,** 40–48.
21. Kodis, G., Herrero, C., Palacios, R., Mariño-Ochoa, E., Gould, S., de la Garza, L., van Grondelle, R., Gust, D., Moore, T. A., Moore, A. L. & Kennis, J. T. M. (2004) *J. Phys. Chem. B* **108,** 414–425.
22. Mariño Ochoa, E. (2002) Ph.D. thesis (Arizona State University, Tempe).
23. Zigmantas, D., Hiller, R. G., Sharples, F. P., Frank, H. A., Sundstrom, V. & Polivka, T. (2004) *Phys. Chem. Chem. Phys.* **6,** 3009–3016.
24. Herek, J. L., Wendling, M., He, Z., Polivka, T., Garcia-Asua, G., Cogdell, R. J., Hunter, C. N., van Grondelle, R., Sundström, V. & Pullerits, T. (2004) *J. Phys. Chem. B* **108,** 10398–10403.
25. Gradinaru, C. C., van Grondelle, R. & van Amerongen, H. (2003) *J. Phys. Chem. B* **107,** 3938–3943.
26. van Stokkum, I. H. M., Larsen, D. S. & van Grondelle, R. (2004) *Biochim. Biophys. Acta* **1657,** 82–104.
27. Frank, H. A., Bautista, J. A., Josue, J., Pendon, Z., Hiller, R. G., Sharples, F. P., Gosztola, D. & Wasielewski, M. R. (2000) *J. Phys. Chem. B* **104,** 4569–4577.
28. Papagiannakis, E., Larsen, D. S., van Stokkum, I. H. M., Vengris, M., Hiller, R. G. & van Grondelle, R. (2004) *Biochemistry* **43,** 15303–15309.
29. Palacios, M. A., Frese, R. N., Gradinaru, C. C., van Stokkum, I. H. M., Premvardhan, L. L., Horton, P., Ruban, A. V., van Grondelle, R. & van Amerongen, H. (2003) *Biochim. Biophys. Acta* **1605,** 83–95.
30. Bautista, J. A., Connors, R. E., Raju, B. B., Hiller, R. G., Sharples, F. P., Gosztola, D., Wasielewski, M. R. & Frank, H. A. (1999) *J. Phys. Chem. B* **103,** 8751–8758.
31. Mathies, R. & Stryer, L. (1976) *Proc. Natl. Acad. Sci. USA* **73,** 2169–2173.
32. Ruban, A. V., Pascal, A., Lee, P. J., Robert, B. & Horton, P. (2002) *J. Biol. Chem.* **277,** 42937–42942.
33. Polivka, T., Herek, J. L., Zigmantas, D., Akerlund, H. E. & Sundström, V. (1999) *Proc. Natl. Acad. Sci. USA* **96,** 4914–4917.
34. Polivka, T., Zigmantas, D., Sundström, V., Formaggio, E., Cinque, G. & Bassi, R. (2002) *Biochemistry* **41,** 439–450.
35. Ruban, A. V., Pascal, A. A., Robert, B. & Horton, P. (2002) *J. Biol. Chem.* **277,** 7785–7789.
36. Hermant, R. M., Liddell, P. A., Lin, S., Alden, R. G., Kang, H. K., Moore, A. L., Moore, T. A. & Gust, D. (1993) *J. Am. Chem. Soc.* **115,** 2080–2081.
37. Gradinaru, C. C., Kennis, J. T. M., Papagiannakis, E., van Stokkum, I. H. M., Cogdell, R. J., Fleming, G. R., Niederman, R. A. & van Grondelle, R. (2001) *Proc. Natl. Acad. Sci. USA* **98,** 2364–2369.